Effect of subsurface dams on saltwater intrusion and fresh groundwater discharge

Qinpeng Chang[1,2], Tianyuan Zheng[3*], Xilai Zheng[1,2*], Bo Zhang[1,2], Qiguo Sun[1,2], Marc Walther[4,5]

1. College of Environmental Science and Engineering, Ocean University of China, Qingdao 266100, China

2. Key Laboratory of Marine Environment and Ecological Education, Ocean University of China, Qingdao 266100, China

3. College of Engineering, Ocean University of China, Qingdao 266100, China

4. Technische Universität Dresden, Faculty of Environmental Sciences, Department of Hydrosciences, Institute for Groundwater Management, Professorship for Contaminant Hydrology, 01062 Dresden, Germany

5. Helmholtz-Centre for Environmental Research–UFZ Leipzig, Department of Environmental Informatics, 04318 Leipzig, Germany

Abstract: Subsurface dams are widely used to prevent saltwater intrusion around the world. A subsurface dam blocks the groundwater movement both from and towards the sea. This blockage often leads to an accumulation of pollutants and salt on the inland and sea-side of the dam, respectively. While the latter is intended, the former effect is not desired and poses a huge problem in groundwater management. Herein, we propose the use of dams of minimum effective height to prevent saltwater intrusion, and the use of the fresh groundwater discharge to assess the environmental

* Corresponding author: Dr. Tianyuan Zheng; phone: +86-532-6678-1020; email: zhengtianyuan@ouc.edu.cn
* Corresponding author: Dr. Xilai Zheng; phone: +86-532-6678-1759; email: zhxilai@ouc.edu.cn

performance of the subsurface dam. Laboratory tests and numerical simulations were used to study the effects of dam height, distance from the saltwater boundary, and head difference on the subsurface dam's saltwater intrusion prevention efficiency and fresh groundwater discharge. We found that i) the fresh groundwater discharge reaches its peak at the minimum dam effective height, and ii) the minimum effective dam height is shorter than the height of SWI without the dam. This means, under the premise of effectively preventing SWI, we can reduce both construction costs and increase fresh groundwater discharge through constructing the dam with the minimum effective dam height. When the dam height was less than the minimum effective dam height, the subsurface dam had little effect in preventing saltwater intrusion. As the dam distance to the shoreline increased, the minimum effective dam height and the peak fresh groundwater discharge decreased simultaneously. A reduction of the dam height is conducive to saving engineering cost, while a reduction of the peak fresh groundwater discharge favors the accumulation of land-based pollutants and salt. Although an increased distance of the dam to the coast seems more economic during construction, this also implies a larger inland soil salinization and accumulation of pollutants. The site selection of subsurface dams is therefore an optimization task that should consider both the engineering cost and ecological environmental effects.

Key word: saltwater intrusion; subsurface dams; dam location; minimum effective dam height; fresh groundwater discharge

1. Introduction

Saltwater intrusion (SWI) is the primary adverse factor affecting groundwater exploitation in coastal regions (Bear, 1999; Kayode, 2017). Under the action of a regional groundwater flow field, fresh groundwater discharges to the ocean and exchanges with the high-density saltwater body near the coast (Fig. 1a). Excessive pumping of groundwater in coastal aquifers leads to a decreased water table height, and the saltwater wedge keeps invading inland (Goswami, 2007; Walther et al., 2017; Zhang, 2019). SWI directly leads to soil salinization and to the substantial decline of agricultural output (Yu, 2019). SWI has become an important factor restricting the social and economic development in coastal regions (Werner et al., 2013).

At present, the main methods to prevent SWI are hydraulic barriers and physical barriers (Abarca et al., 2006; Botero-Acosta and Donado, 2015). In addition, the compressed air injection method was proposed to prevent SWI; but it has not been widely used due to its low efficiency for preventing SWI (Sun et al., 2013). Hydraulic barriers require the continuous pumping of the saltwater or recharge of the fresh water into the aquifers, and the wells used, face the problem of clogging in the long run (Luyun et al., 2011; Allow, 2012). Physical barriers use the “soil mixing wall method” or “trench-cutting remixing deep wall method” to construct impervious soil-cement-bentonite walls that can effectively prevent SWI once and for all (Onder et al., 2005; Luiz et al., 2018).

Since the 1980s, Japan, China, India, the Middle East, and African countries have built many underground physical barriers to prevent and control SWI (Raju et al., 2013; Stevanović 2015). At present, physical barriers can be divided into cut-off walls, subsurface dams, and semi-pervious subsurface barriers (SPSB) (Fig. 1-b, c, and d) (Hasan Basri, 2001; Kaleris and Ziogas, 2013). Subsurface dams are the most widely used wall type in the international field of preventing SWI (Nawa et al., 2009; Abdoulhalik et al., 2017c; Jamali et al. 2018). Jamali et al. (2013) used a GIS model coupled to a groundwater balance model to study the siting solution of subsurface dams. Kang et al. (2017) used isotope analysis to investigate the effect of subsurface dams on the groundwater nutrient dynamics in the Wang River watershed in China. They found that due to the blocking effect of subsurface dams on the groundwater, the nitrogen and phosphorus concentrations upstream of the subsurface dams were higher than those downstream. Cantalice et al. (2016) built an underground dam in the Brazilian Jacu watershed and monitored the soil moisture, groundwater quality, and electrical conductivity for more than three years. According to the monitoring results, the underground dam resulted in the retention of more soil moisture in the rainy season. However, the interception effect of the underground dam led to gradual increase of groundwater salinity upstream, which eventually lead to soil salinization. Senthilkumar and Elango (2011) used MODFLOW to study the influence of subsurface dams on groundwater flow fields in the Palar River basin in India. The model predicted that after the establishment of subsurface dams, the upstream groundwater levels would rise by 0.1–0.3 m, and the range of influence would be about 1.5–2 km upstream, while the downstream groundwater level would decrease by 0.1–0.2 m. Abdoulhalik and Ahmed (2017a) used laboratory tests and SEAWAT numerical simulation to study the cut-off wall efficiency for SWI control in stratified aquifers. They combined, for the first time, the use of cut-off walls and subsurface dams to enhance the efficiency of SWI prevention (Abdoulhalik et al., 2017b). Luyun et al. (2009) studied the relationship between the height of subsurface dams and the thickness of the saltwater wedge using laboratory tests and SEAWAT. They found that when the subsurface dams were higher than the thickness of the saltwater wedge, seawater intrusion could be prevented, and the saltwater trapped upstream could be flushed out. However, the effects of the construction location of subsurface dams and head difference were neglected. The efficiency of subsurface dams for preventing SWI is determined by a wall's depth, hydraulic conductivity, distance from the coast, groundwater velocity, and aquifer anisotropy (Kaleris and Ziogas, 2013).

The top of a subsurface dam is generally at sea level (Fig. 1-c). In some regions, the subsurface dams intersect the full cross-section of the aquifer to store water underground for irrigation（Fig. 1-d）(Silva et al., 1998; Ishida et al., 2011; Yasumoto et al., 2011). However, the excessive dam height will not only increase the engineering cost, but will also cut off the route of fresh groundwater discharge to the sea. The interception of fresh groundwater leads to inland soil salinization and accumulation of pollutants (see references above). In order to avoid such disadvantages, Sugio et al., (1987) proposed to change impermeable subsurface dams to semi-permeable ones. Then the salt and pollutants in the fresh groundwater could discharge to the sea through the semi-permeable subsurface dam. However, the saltwater could also invade the aquifer through the semi-permeable subsurface dam, which reduced the efficiency of the subsurface dam for preventing SWI. In conclusion, it is a significant problem to prevent the inland soil salinization and accumulation of pollutants by maximizing the fresh groundwater discharge, while ensuring the efficiency of subsurface dams for preventing SWI.

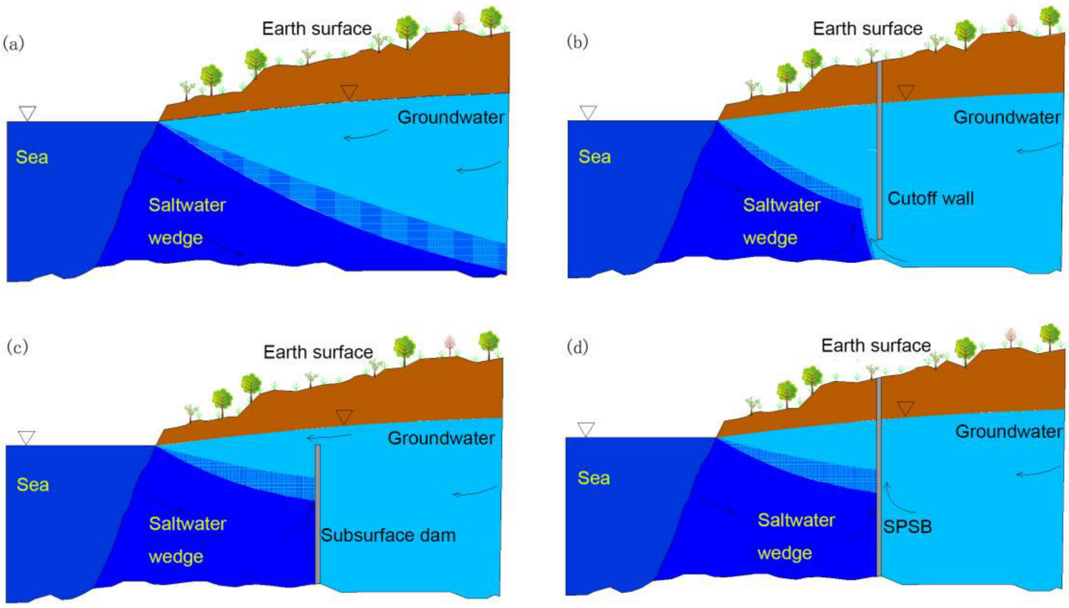

Fig. 1. Schematic diagrams of SWI and physical barriers (a) SWI; (b) Cutoff wall; (c) Subsurface dam; (d) Semi-pervious subsurface barrier (SPSB).

In contrast to previous work, we propose using dams of minimum effective height to prevent SWI. Moreover, we used the fresh groundwater discharge to assess the environmental performance of the subsurface dam, as an increased fresh groundwater discharge is beneficial for carrying land-based pollutants and salt to the sea, which accumulate in traditional high subsurface barriers (Qu et al., 2017; Sathe and Mahanta, 2019; Tavakoli-Kivi et al., 2019; Sun et al., 2019). We used laboratory tests and numerical simulation to investigate the optimization of subsurface dams. The laboratory tests were completed in a flow tank to represent SWI in an unconfined aquifer under the influence of a subsurface dam. SEAWAT was used to interpret the laboratory test results. The subsurface dam height, dam distance to the saltwater boundary, and head difference were investigated to maximize the efficiency of SWI prevention and the discharge of fresh groundwater to the sea. We have found that the fresh groundwater discharge reaches its peak with the minimum effective dam height and the minimum effective dam height is slightly shorter than the height of SWI without the dam. Thus, we can reduce both construction costs and increase fresh groundwater discharge through constructing the dam with the optimized dam height.

Table 1

Symbols.

c_f	freshwater concentration [ML^{-3}]
c_s	saltwater concentration [ML^{-3}]
D	molecular diffusion coefficient [L^2T^{-1}]
dh	head difference of freshwater and saltwater [L]
H_{aqu}	aquifer thickness [L]
H_{dam}	subsurface dam height [L]
H_{min}	minimum effective dam height to prevent SWI [L]
h_f	freshwater level [L]
h_s	Saltwater level [L]

K	hydraulic conductivity [LT^{-1}]
L_{dam}	dam distance from the saltwater boundary [L]
L_{SWI}	length of the saltwater wedge [L]
Q	discharge of fresh groundwater to the sea when SWI reaches dynamic equilibrium [L^3T^{-1}]
α_L	longitudinal dispersivity [L]
α_T	transverse dispersivity [L]
ρ_f	freshwater density [ML^{-3}]
ρ_s	saltwater density [ML^{-3}]

2. Material and methods

2.1. Scenario definition

We defined two scenarios to investigate the efficiency of the subsurface dam. A baseline case was used to compare the experimental and numerical setups and acquire a parametrization. In the baseline case, the head differences of freshwater and saltwater were set as 8mm, 9mm and 10mm in the lab experiments. Length of saltwater wedge dynamics were used to compare the lab results and numerical simulations.

A subsurface dam case was used to assess the sensitivity of the dam height, location, and head difference with respect to steady-state SWI length and fresh groundwater discharge. The subsurface dam case was defined as: The base dam case was set as dam height = 7 cm, distance = 20 cm, and head difference = 9 mm. We changed one factor of dam height, location, and head difference at a time in the lab experiments to compare with the base dam case. Pictures of steady-state SWI were taken to observe the shape of saltwater wedge at different dam cases. SEAWAT was used to assess the sensitivity of the dam height, location, and head difference.

2.2. Laboratory Material

The experiment was carried out in a flow tank with internal dimensions of 90 cm (length) × 45 cm (height) × 5 cm (width) (Fig. 2). In order to simulate an unconfined aquifer, the water tank was divided into three zones by porous plates, freshwater reservoir, saltwater reservoir, and porous media chamber. Glass beads with uniform diameter of 0.7 mm were used to fill in the middle zone of the tank as porous media. The fresh and saltwater reservoirs were positioned on the left and right sides of the flow tank, respectively, and the fresh and saltwater flow was pumped at a constant rate into the reservoirs from the bottom inlets. The constant heads of the fresh groundwater and saltwater were controlled by adjustable drainage overflow pipes.

NaCl solution with a concentration of 36 g/L was prepared to represent seawater. A densitometer (AlfaMirage SD-200L) was used to measure the seawater density (ρ_s) = 1025 Kg/m^3, the freshwater density (ρ_f) = 1000Kg/m^3. Cochineal dyes (red food color, Sinopharm Chemical Reagent Co.,Ltd) were added to trace the saltwater. The dyes could be migrated synchronously with the saltwater in the flow tank (Goswami et al., 2007). Therefore, the red area in the flow tank could be used to determine the range of the saltwater wedge. The average hydraulic conductivity (K) of the porous media, as calculated by Darcy's law, was 5.8 E-3 m/s, and the porosity measured by the volume method was 0.4. The longitudinal dispersivity (α_L) is 0.13cm, which was determined by fitting the breakthrough curves with an one-dimensional column test. The transverse dispersivity (α_T) was set to be 1/10 of the longitudinal dispersion (Shoemaker et al., 2004 ; Lu et al., 2013). The subsurface dam was made of plasticine which is impermeable.

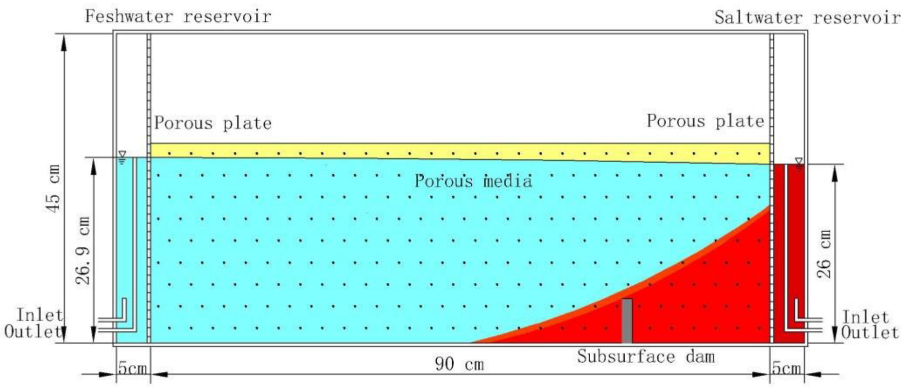

Fig. 2. Schematic diagram of the laboratory setup.

2.3. Experimental setup

The saltwater head was fixed at 26 cm, the fresh groundwater head was adjustable, and was adjusted to 26.8 cm, 26.9 cm, and 27.0 cm, respectively, during different scenarios. We filled the glass beads into the porous media chamber layer-by-layer under saturated conditions to avoid air bubbles to reside in the pores. The fresh water was pumped into the freshwater reservoir, which was then filled with porous media and the overflow discharged through the overflow outlet of the saltwater reservoir. Then the saltwater entered the saltwater reservoir from the inlet pipe and gradually filled the saltwater reservoir from the bottom up. The saltwater wedge gradually formed and began a continuous invasion of the aquifer. The position of the saltwater wedge was recorded every 10 min by a digital camera (Canon IXUS 285 HS). As soon as the saltwater wedge reached the subsurface dam, it stopped advancing and rose against the subsurface dam. If the saltwater wedge could be captured at the position of the subsurface dam, the dam was effective to prevent SWI. If the saltwater extended downward behind the dam after flowing over the top of the subsurface dam, the subsurface dam failed to prevent SWI. When the saltwater reached the impervious base behind the dam, a new saltwater wedge formed and continued to invade the aquifer. We considered the setup equilibrated when SWI was not advancing more than 1 mm per 10 minutes.

2.4. Numerical setup

SEAWAT was used to simulate SWI and to calculate the fresh groundwater discharge to the sea (Guo and Langevin, 2002; Langevin, 2003). During the setup of the numerical model, we followed the laboratory settings and parameters as close as possible. The numerical simulation area was a homogeneous, unconfined, two-dimensional, vertical cross section with the size of 90 × 27 cm^2. A no-flow boundary condition was defined on the upper part and lower part of the numerical model. The left-side freshwater boundary was set as a variable constant head boundary (26.5 to 27.1 cm); the concentration was set to c_f = 0 g/L. The right-side saltwater boundary was set to a constant head of 26 cm, and the concentration was set to c_s = 36 g/L.

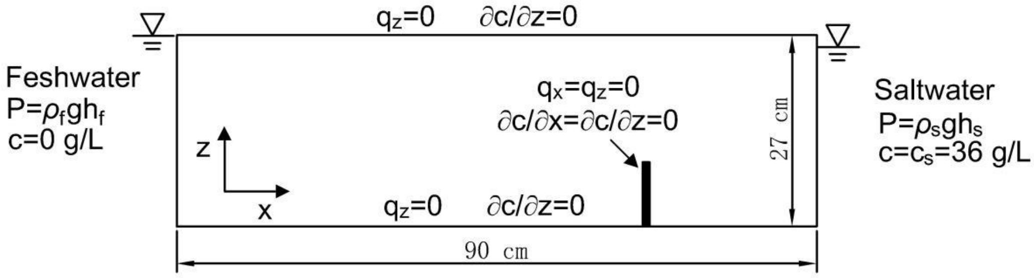

Fig. 3. Model domain and boundary conditions for the numerical simulations.

The simulation area was discretized by a uniform grid with quadratic elements with an edge length of 0.5 cm. The grid spacing and dispersivity satisfied the Péclet number criterion to ensure numerical stability (Voss et al., 1987):

$$\mathrm{Pe} = \frac{v\Delta \mathrm{L}}{\mathrm{D} + \alpha_{\mathrm{L}}\, v} \approx \frac{\Delta \mathrm{L}}{\alpha_{\mathrm{L}}} = 3.8 < 4 \tag{1}$$

Where ΔL is the grid spacing, D is molecular diffusion. The time step was set to 60 s. The aquifer medium hydraulic conductivity (K) was set to 5.8E-3 m/s. As the used plasticine is practically impermeable, the hydraulic conductivity of the subsurface dam was set to 1E-9 m/s, and the width of the subsurface dam was 1 cm. A stress period was set for both the baseline case and the subsurface dam case, lasting for 6 h, which was adequate for the saltwater wedge to reach a state of dynamic equilibrium.

3. Results and discussion

3.1. Baseline case

In the baseline case, we firstly studied the influence of the variation of the head difference. Fig. 4-a, b, and c shows the results for head differences of 8, 9, and 10 mm which resulted in intrusion lengths of the saltwater wedge of 56.4, 44.7, and 37.1 cm, respectively. Fig. 4-d shows the comparison of the 50% isoline under the different head conditions. 50% isoline is wildly used for saltwater wedge in the aquifer with low dispersivity (Goswami et al., 2007; Luyun et al., 2009; Stoeckl et al.,2016).

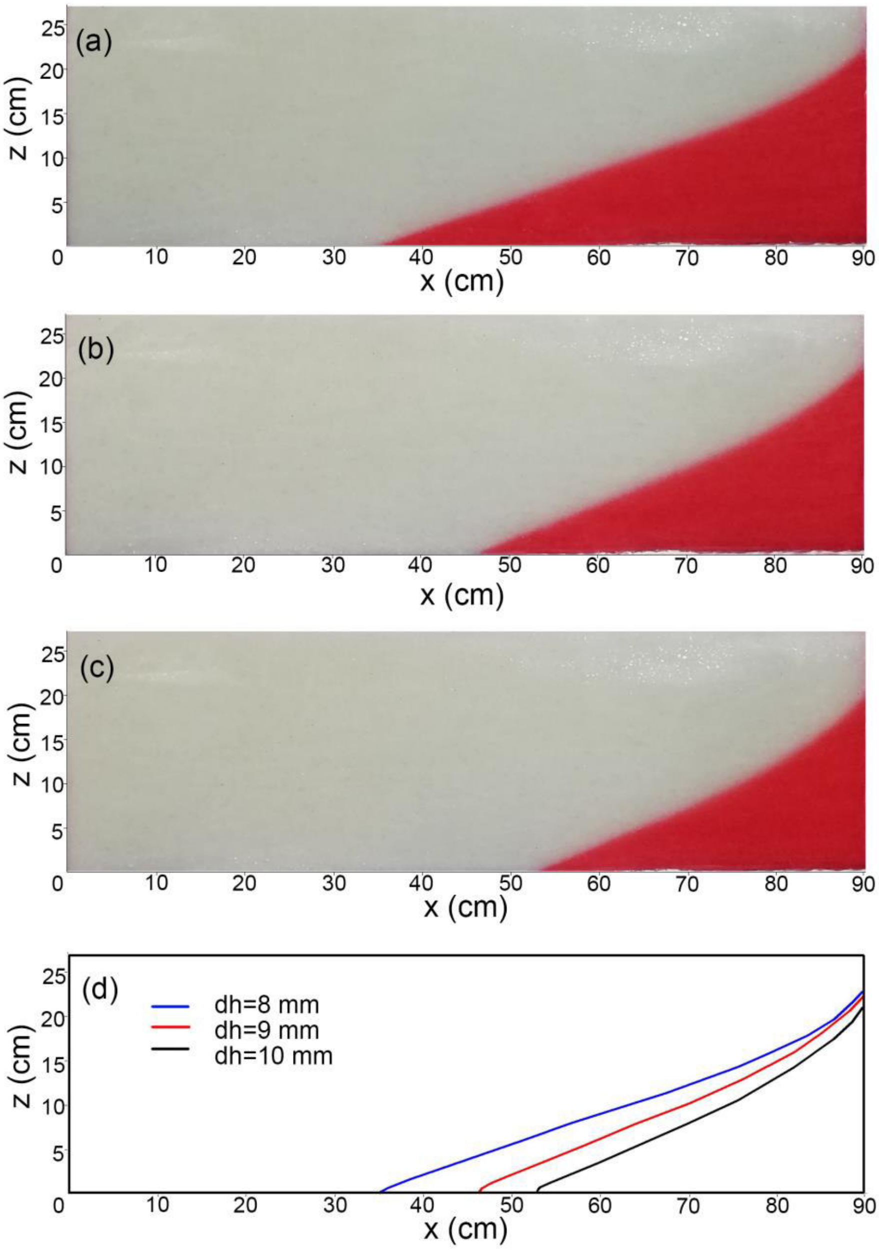

Fig. 4. Photographs of the steady-state saltwater wedge with head difference of (a) 8 mm, (b) 9 mm, (c) 10 mm, and (d) comparison of the 50% isoline.

The comparison between the experimental data and the numerical simulation results of the length of the saltwater wedge is shown in Fig. 5. The numerical simulation results and the experimental data have a good degree of fit under the different head conditions. For the head differences of 8, 9, and 10 mm, SWI reaches dynamic equilibrium at 300, 230, and 180 min, respectively.

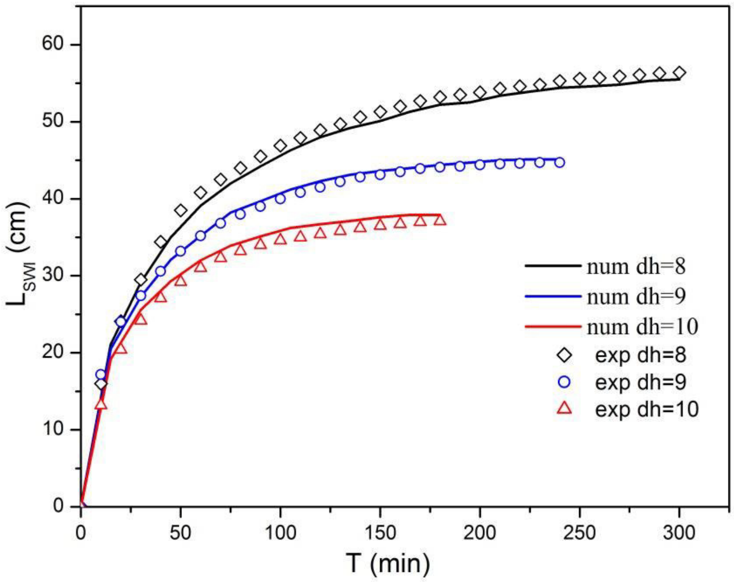

Fig. 5. Comparison between transient experimental and numerical length of saltwater wedge (L_{SWI}) with different head differences.

The water flowing out of the right boundary of the flow tank is the brackish water mixed with the fresh groundwater and saltwater. Therefore, the study on the fresh groundwater discharge should be based on the water balance of the fresh groundwater flowing into and flowing out of the flow tank. SEAWAT was used to calculate the fresh groundwater rate flowing into the flow tank, which is equal to the discharge of the fresh groundwater. Fig. 6 plots the variation of fresh groundwater discharge versus head difference when SWI reaches dynamic equilibrium. It can be seen that the fresh groundwater discharge increased gradually with increase of the head difference. This is because the velocity of the fresh groundwater flowing into the flow tank increases with increase of the head difference according to Darcy's law. The increased fresh groundwater flow velocity results in an increase of the fresh groundwater discharge .

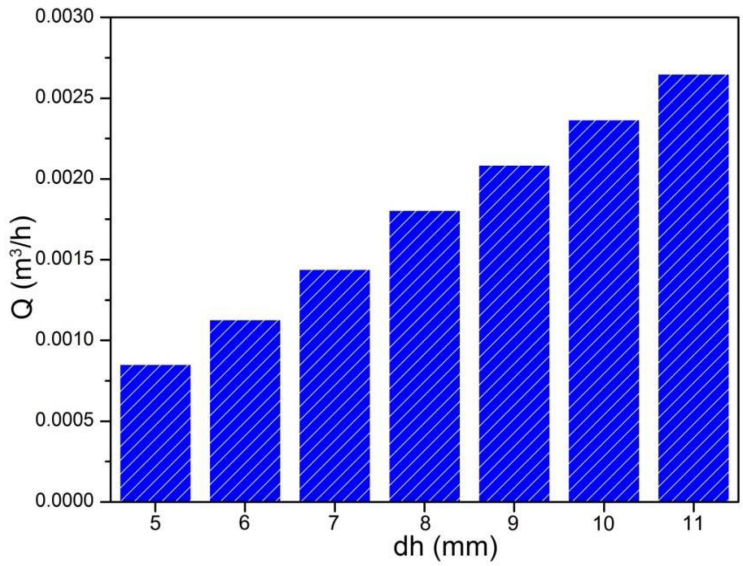

Fig. 6. Discharge of fresh groundwater with different head differences .

3.2. Dam height

The head difference of freshwater boundary and saltwater boundary was kept at 9 mm. The location of the subsurface dam was set at a distance of 20 cm from the saltwater boundary. The subsurface dam heights were set at 6 cm, 7 cm, and 8 cm, respectively. Fig. 7 shows the results for the variations of the dam height with the laboratory experiments. In the case of no subsurface dam, the length of the saltwater wedge was 44.7 cm (Fig. 3-b). When the dam height was 6 cm, the saltwater wedge flowed over the top of the subsurface dam and advanced to a distance of 43.3 cm. In this case, the subsurface dam lost its function of preventing SWI. When the dam height was increased to 7 cm, the saltwater wedge was intercepted at the position of the subsurface dam, and the thickness of the saltwater wedge at the dam was approximately equal to the height of the subsurface dam. When the dam height was increased to 8 cm, the saltwater wedge was also effectively intercepted, and the thickness of the saltwater wedge toe was lower than the height of the subsurface dam.

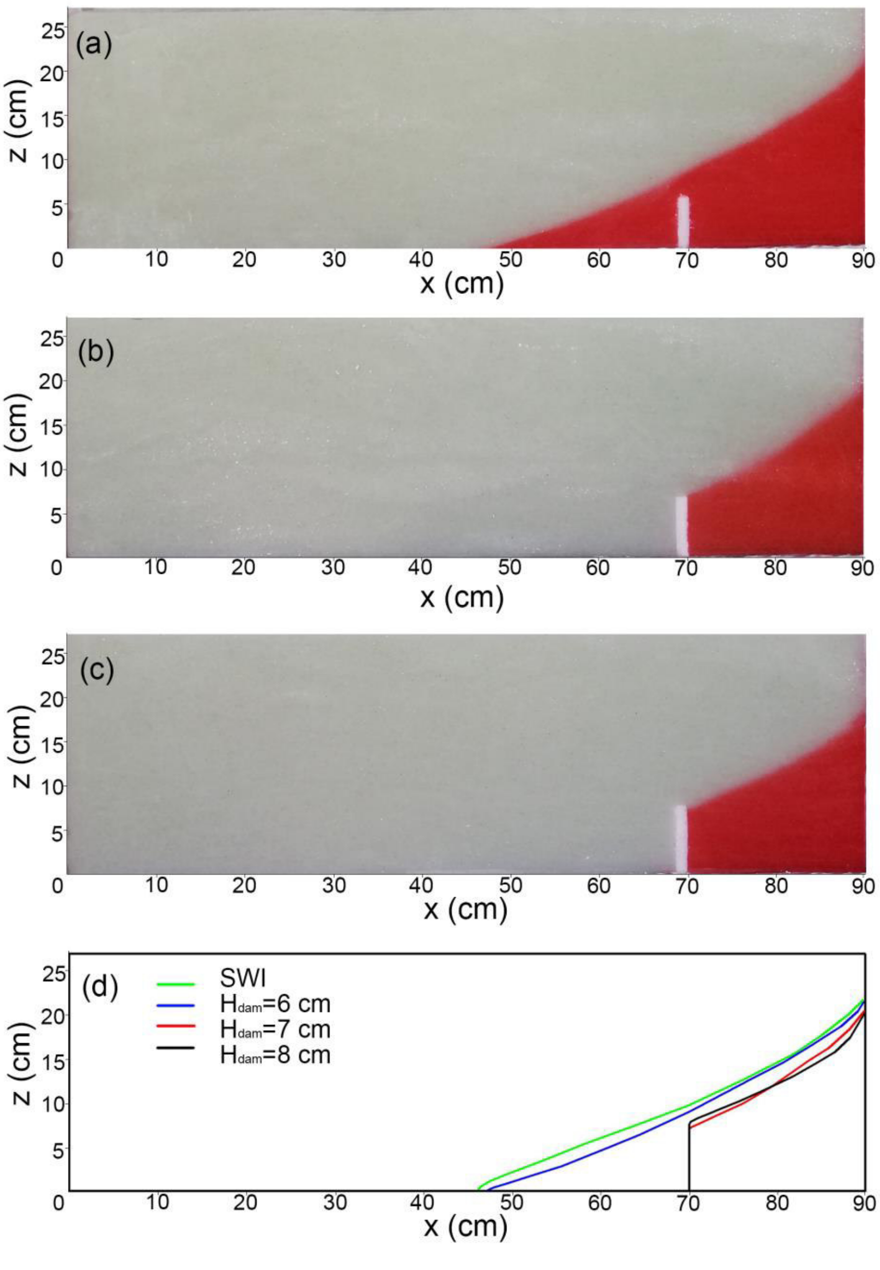

Fig. 7. Photographs of the steady-state saltwater wedge in a head difference of 9 mm, with dam heights of (a) 6 cm, (b) 7 cm, and (c) 8 cm, and (d) comparison of the 50%

isoline, SWI is equivalent to dh = 9mm in fig. 3.

The numerical simulation results and the laboratory tests have a good degree of fit in Fig.7 and Fig.8, which shows the numerical simulations are reliable. For the dam heights of 6, 7, and 8 cm, the saltwater wedge reaches dynamic equilibrium at 463, 54, and 64 min, respectively. Comparing with the SWI dynamic equilibrium time of 230min without the dam, the equilibrium time decreases three quarters when the subsurface dam is effective. Even if the subsurface dam is too low to prevent SWI, it can still slow down the speed of SWI.

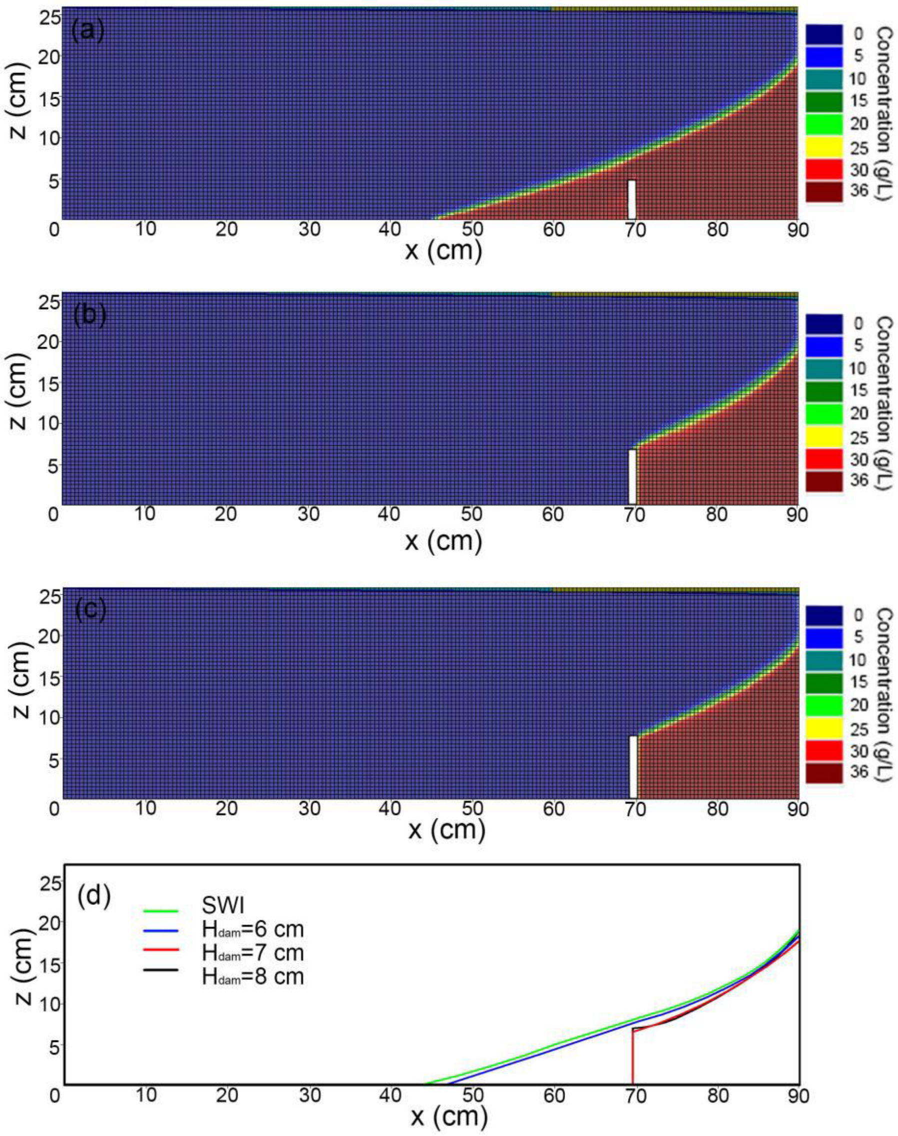

Fig. 8. The numerical simulations of the steady-state saltwater wedge in a head difference of 9 mm, with dam heights of (a) 6 cm, (b) 7 cm, and (c) 8 cm, and (d) comparison of the 50% isoline, SWI is equivalent to dh = 9mm.

In the following, we use the dimenionsless ratio of the dam height H_{dam} and the aquifer thickness H_{aqu} (H_{aqu} =26cm). Fig. 9 shows the influence of the dam height on the SWI length. Until the ratio H_{dam}/H_{aqu} reaches 0.27 (i.e. H_{dam} = 7 cm), the SWI length decreases only slightly and is similar to the baseline case, indicating that the dam loses the function of preventing SWI. When H_{dam}/H_{aqu} is larger than 0.27, the SWI length decreases sharply to 20 cm, and the saltwater wedge is intercepted by the dam. Thus, H_{dam}/H_{aqu} = 0.27 is the minimum effective dam height to prevent SWI in the case of a head difference of 9 mm.

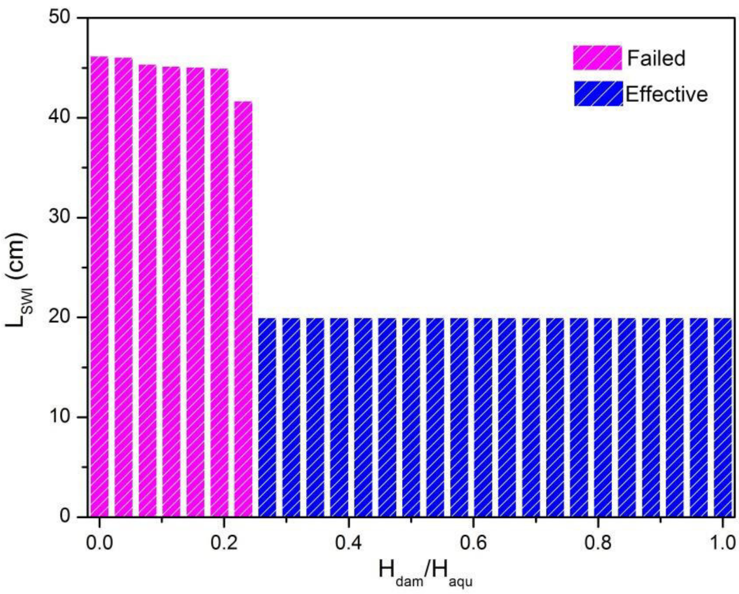

Fig. 9. Length of saltwater wedge with different dam height ratios. The purple bars represent dam heights that failed to prevent SWI; the blue bars represent dam heights with effective blocking of SWI.

Fig. 10 shows the fresh groundwater discharge for different dam heights. With increase of the dam height, the fresh groundwater discharge increases slightly and then decreases sharply. The fresh groundwater discharge reaches the maximum value at H_{dam}/H_{aqu} = 0.27. From Fig. 9, we know that H_{dam}/H_{aqu} = 0.27 is the minimum effective dam height to prevent SWI in this case. It is worth noting that the fresh groundwater discharge at the minimum effective dam height is larger than that of the baseline case (without subsurface dam). The flow velocity in the saltwater wedge is far smaller than that of fresh groundwater (Abdoulhalik and Ahmed, 2017a). Therefore the stagnant saltwater wedge decreases the discharge section area just like the subsurface dam does. As we can see in Fig. 7d, the thickness of the saltwater wedge in the baseline case (without subsurface dam) is higher than the minimum effective dam height at the dam location. This means that the fresh groundwater discharge section area in the baseline case is smaller than that of the minimum effective dam case. At the same height as sea level, the fresh groundwater discharge of the subsurface dam decreases to 37.2% of the maximum value. This is because the fresh groundwater discharge section area is too small.

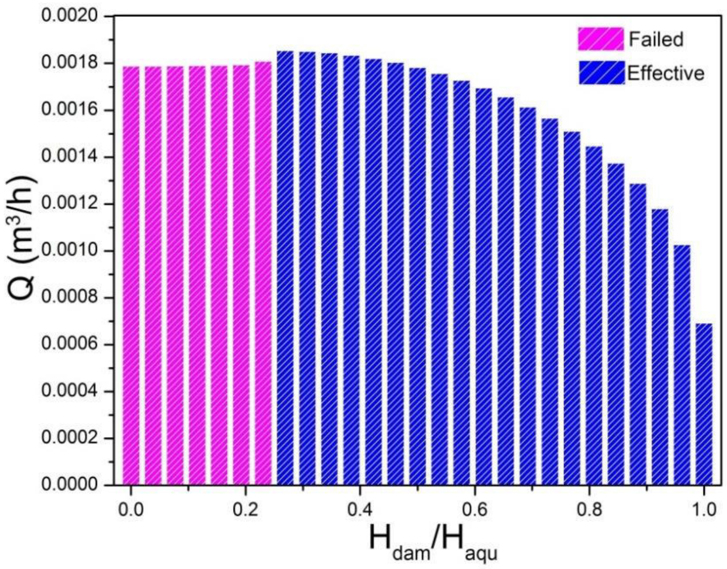

Fig. 10. Discharge of fresh groundwater with different dam height ratios. Purple bars represent failed SWI prevention; blue bars represent effective SWI prevention.

3.3. Dam Location

Under the condition that the head difference was 9 mm, and the dam height was set at 7 cm (i.e. the minimum height at which the dam was effective), the distance from the saltwater boundary was changed to 15 cm, and 25 cm. According to the laboratory results, when the distance from saltwater boundary was 15 cm, the saltwater wedge crossed the top of the subsurface dam and advanced to a length of 42.8 cm (Fig. 11 a). When the distance was increased to 25 cm, the subsurface dam could still prevent SWI (Fig. 11 b).

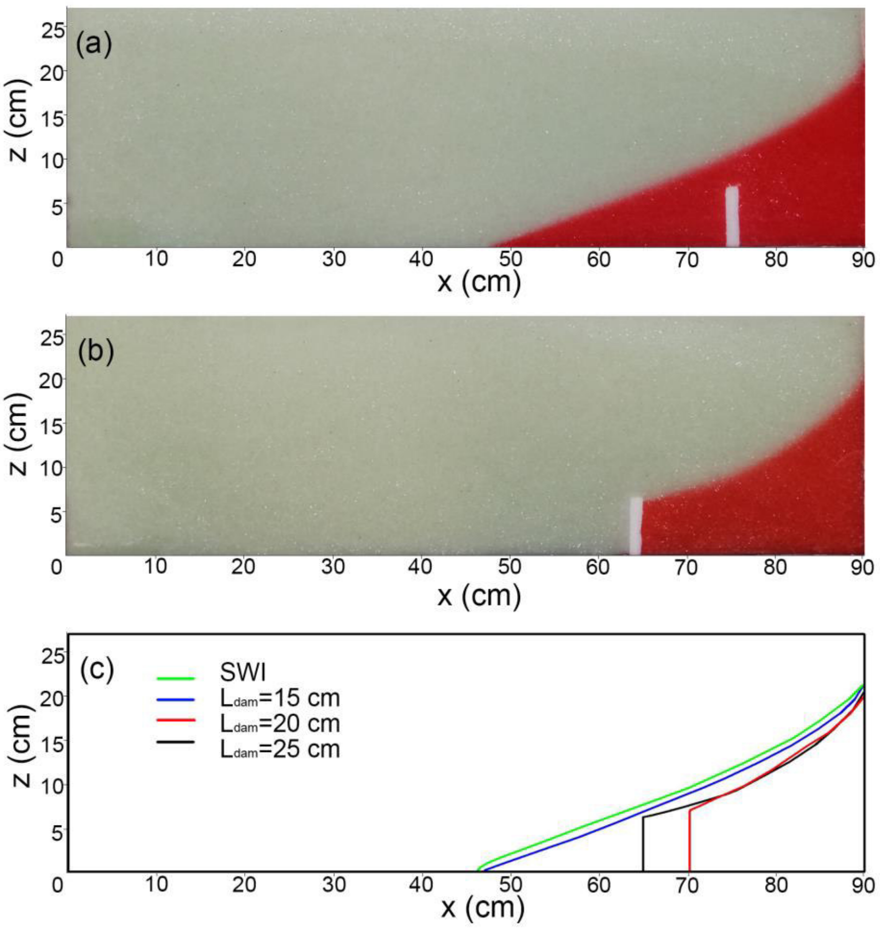

Fig. 11. Photographs of the steady-state saltwater wedge in a head difference of 9 mm with distance from saltwater boundary of (a) 15 cm, (b) 25 cm, and (c) comparison of the 50% isoline, SWI is equivalent to dh = 9mm in fig. 3.

Fig. 12 shows the influence of the dam location on the saltwater wedge length. The dam location is expressed by the ratio of the distance from saltwater boundary L_{dam} to the thickness of the aquifer H_{aqu}. When L_{dam}/H_{aqu} is less than 0.77 (L_{dam} = 20 cm), the saltwater wedge length decreases slightly with increase of L_{dam}/H_{aqu}. When L_{dam}/H_{aqu} is equal to 0.77, the saltwater wedge length sharply decreases to 20 cm, indicating that the saltwater wedge is intercepted by the subsurface dam. When L_{dam}/H_{aqu} is greater than 0.77, the saltwater wedge is still intercepted at the dam position. The saltwater wedge length increases with the dam distance from the saltwater boundary. Therefore, the minimum effective dam height is related to the distance from the saltwater boundary. Therefore, H_{dam}/H_{aqu} = 0.27 (H_{dam} = 7 cm) is the minimum effective dam height just at the dam position of L_{dam}/H_{aqu} = 0.77 (L_{dam} = 20 cm).

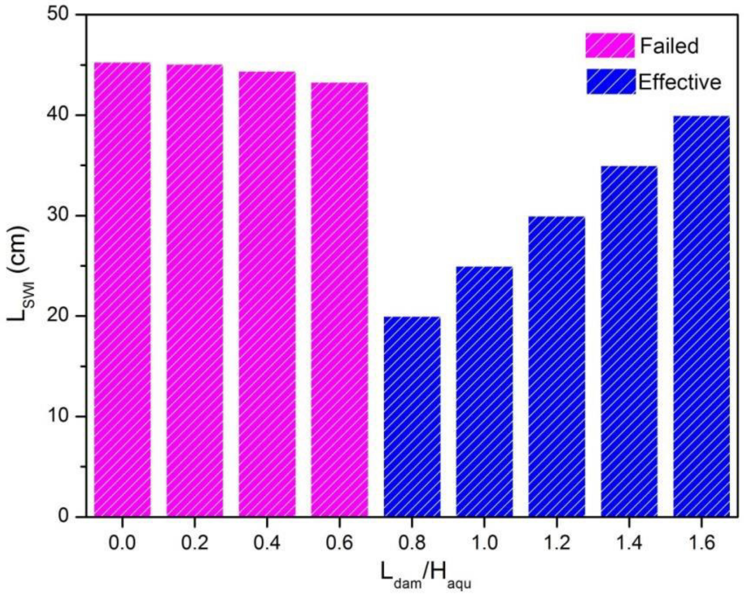

Fig. 12. Length of saltwater wedge at different dam locations. The purple bars represent dam distances that failed to prevent SWI; the blue bars represent dam distances with effective blocking of SWI.

Fig. 13 shows the fresh groundwater discharge in cases with different dam distance. When L_{dam}/H_{aqu} is less than 0.77, the fresh groundwater discharge increases slightly with increase of the dam distance. When L_{dam}/H_{aqu} = 0.77 (L_{dam} = 20 cm), the discharge reaches its peak. When L_{dam}/H_{aqu} is greater than 0.77, the fresh groundwater discharge gradually decreases with increase of the dam distance. As we know from the previous analysis, H_{dam}/H_{aqu} = 0.27 (H_{dam} = 7 cm) is the minimum effective dam height only at the dam position of $L_{dam}/H_{aqu} = 0.77$. Therefore, when $H_{dam}/H_{aqu} = 0.27$ ($H_d = 7$ cm), the discharge reaches the peak at the dam position of $L_{dam}/H_{aqu} = 0.77$ ($L_{dam} = 20$ cm).

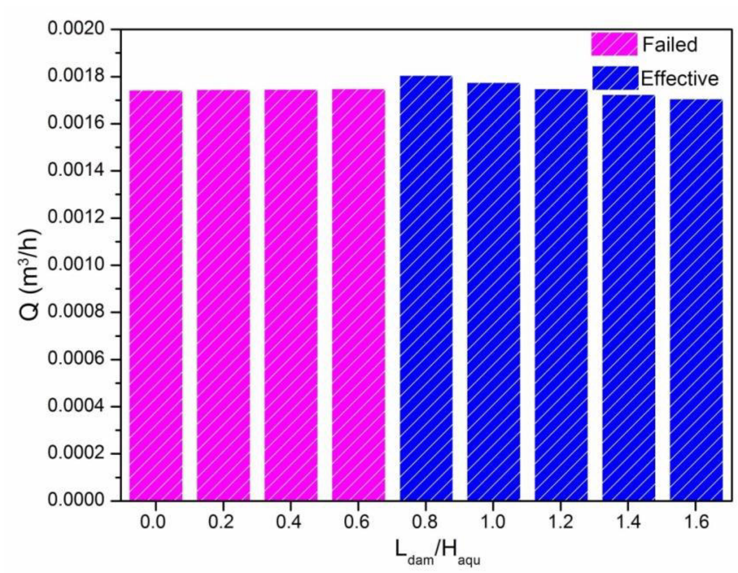

Fig. 13. Discharge of fresh groundwater at different dam locations. Purple bars represent failed SWI prevention; blue bars represent effective SWI prevention.

3.4. Head difference

The hydraulic gradient is expressed by the head difference between the fresh groundwater boundary and the saltwater boundary. The dam height was set at 7 cm, and the distance from the saltwater boundary was set at 20 cm. The head differences were changed to 8 mm and 10 mm, respectively. When the head difference was 8 mm, the saltwater wedge flowed over the top of the subsurface dam and advanced to a length of 53 cm. The subsurface dam could not prevent SWI (Fig. 14 a). When the head difference was increased to 10 mm, the dam height was greater than the thickness of the saltwater wedge toe, and the saltwater wedge stopped at the dam location (Fig. 14 b).

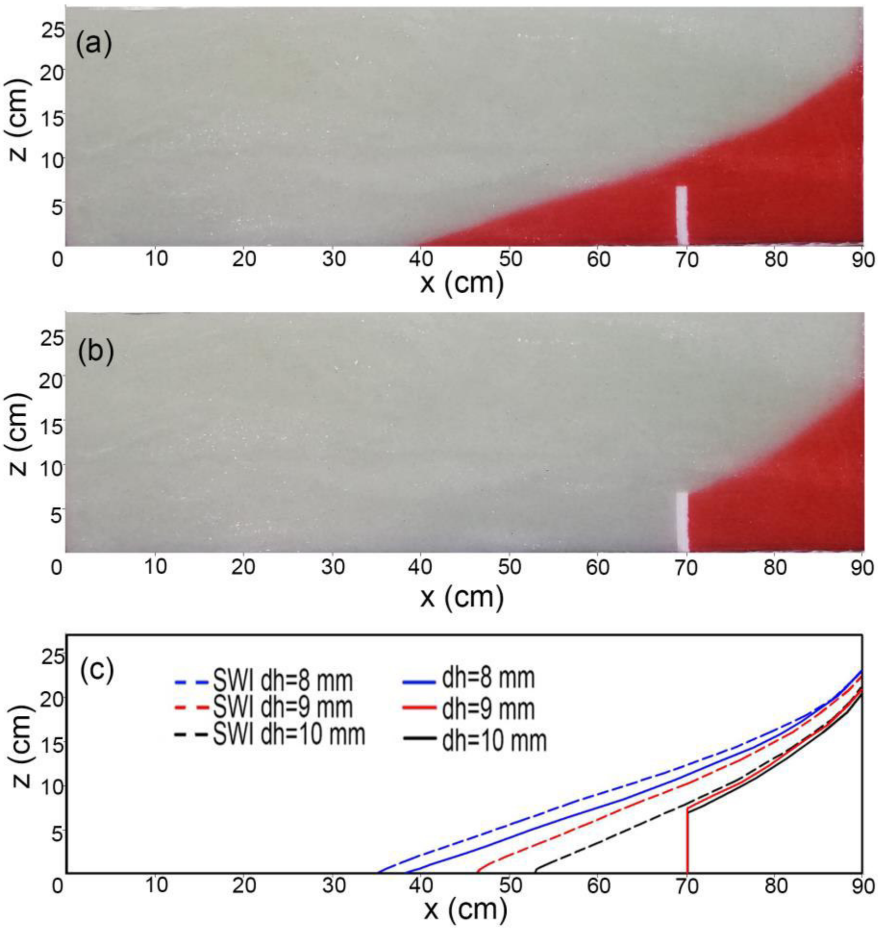

Fig. 14. Photographs of the steady-state saltwater wedge with head difference of (a) 8 mm, (b) 10 mm, and (c) comparison of the 50% isoline, SWI is equivalent to dh = 8, 9, 10mm in fig. 3.

Sensitivity analysis was used to investigate the influence of the head difference on the length of the saltwater wedge (Fig. 15). When the head difference is less than 9mm, the length of the saltwater wedge gradually decreases with the head difference. When the head difference is equal to 9mm, the saltwater wedge sharply decreases to the same distance that the dam is from the shoreline. When the head difference is greater than 9mm, SWI is still intercepted at the dam position.

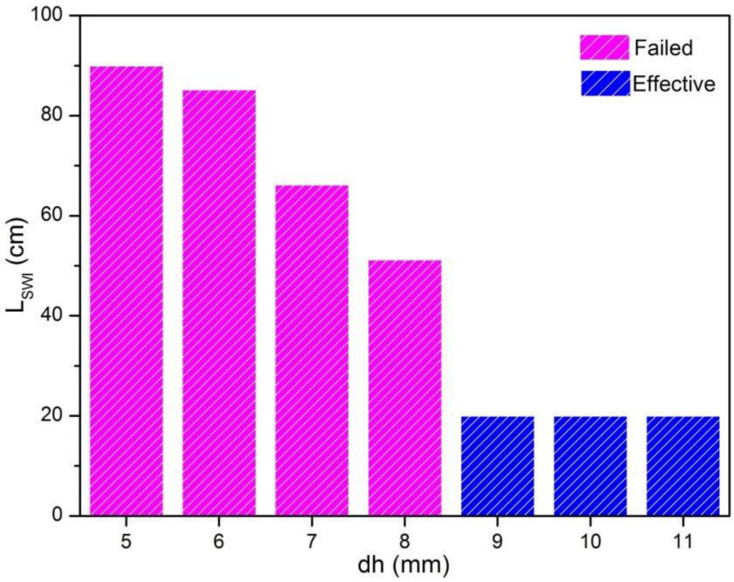

Fig. 15. Length of saltwater wedge with different head differences. The purple bars represent head differences that failed to prevent SWI; the blue bars represent head differences with effective blocking of SWI.

Fig. 16 shows the fresh groundwater discharge in the cases with different head differences. The fresh groundwater discharge gradually increases with the head difference. As we know, the fresh groundwater flow velocity gradually increases with the head difference according to Darcy's law. Therefore, the increase of fresh groundwater flow velocity leads to gradual increase of the fresh groundwater discharge.

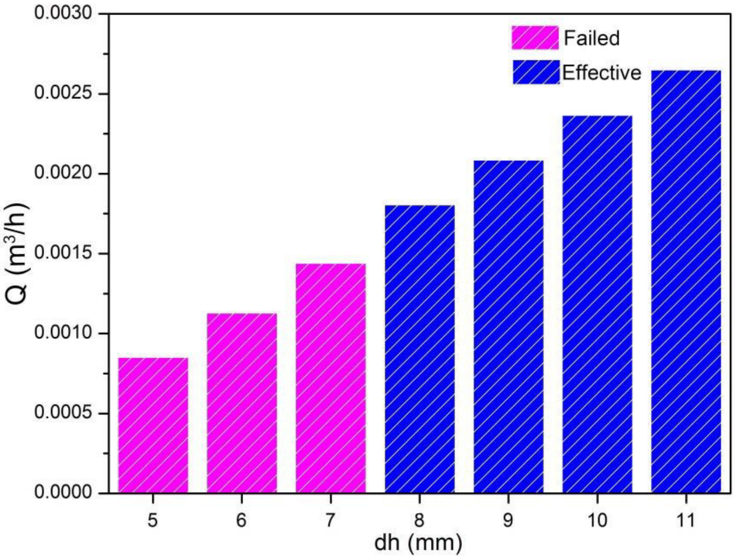

Fig. 16. Discharge of fresh groundwater with different head differences. Purple bars represent failed SWI prevention; blue bars represent effective SWI prevention.

3.5. Discharge at the minimum effective dam height

According to the above analysis, the fresh groundwater discharge is related to the dam height, location, and head difference. Fig. 17 shows the effect of the dam height and location on the fresh groundwater discharge under the head difference of 9mm. As can be seen from Fig. 17, the boundary between the effective region (red region) and the failed region (blue region) is the minimum effective dam height needed to prevent SWI. The discharge reaches its peak value at the minimum effective dam height (H_{min}) at a defined dam position. When the dam distance from the saltwater boundary is zero, the peak discharge is the largest. As the dam distance from the saltwater boundary increases, the peak discharge becomes smaller and smaller.

The fresh groundwater discharge reaches its peak at the minimum effective dam height, which is beneficial to control the accumulation of land-based pollutants and salt. It is of great significance to investigate the minimum effective height of the subsurface dams at different positions and with different head differences.

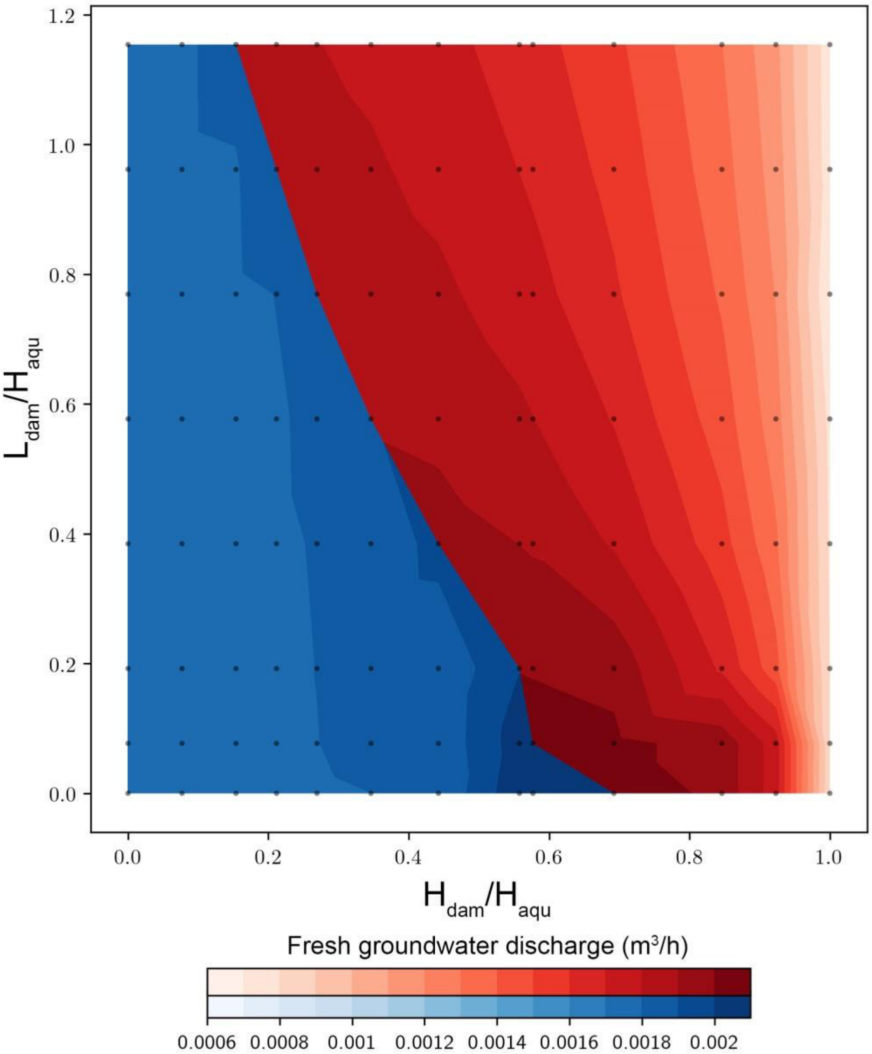

Fig. 17. Effect of the dam location and dam height on the fresh groundwater discharge. Blue region represents failed SWI prevention; red region represents effective SWI prevention.

Fig. 18 shows the minimum effective dam height and corresponding fresh groundwater discharge at the different dam distances and head differences. It can be seen that, with the same head difference, and with increase of the dam distance away from the shoreline, the minimum effective dam height and fresh groundwater discharge decrease gradually. This is consistent with Fig. 17. With increase of the head difference, the minimum effective dam height decreases, and the fresh groundwater discharge increases at the same dam location. This indicates that a large head differences is conducive to saving engineering costs and reducing the accumulation of land-based pollutants and salt.

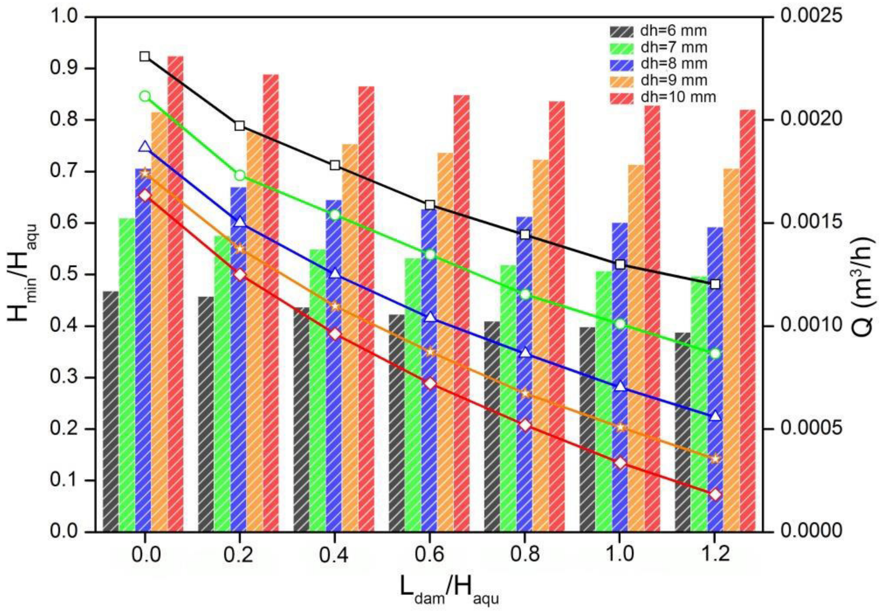

Fig. 18. Discharge of fresh groundwater with dams of the minimum effective height. The lines represent H_{min}/H_{aqu}; the bars represent Q.

4. Summary and conclusions

In this study, we proposed the use of dams of minimum effective height to prevent saltwater intrusion and used the fresh groundwater discharge to assess the environmental performance of the subsurface dam. Laboratory tests and numerical simulations were used to investigate the effects of the dam height, the dam location, and the head difference on the saltwater intrusion prevention ability of the subsurface dam and on the fresh groundwater discharge.

For the baseline case (without subsurface dam), with increase of the head difference, the time for SWI to reach dynamic equilibrium as well as the length of the saltwater wedge shorten, and the fresh groundwater discharge increases.

A minimum effective dam height at a defined distance from the shoreline that will prevent saltwater intrusion could be identified. Until a minimum effective dam height, increasing dam height has no significant effect on decreasing of the saltwater wedge length. When the dam height is equal to or higher than the minimum effective dam height, the saltwater wedge can be intercepted at the subsurface dam position. The fresh groundwater discharge reaches its peak at the minimum effective dam height. A larger freshwater recharge will push back more saltwater. Therefore, the minimum effective dam height is shorter than the height of SWI without the dam. The minimum effective dam height strongly depends on the distance to the shoreline: as the dam distance from saltwater boundary increases, the minimum effective height and the peak fresh groundwater discharge decreases simultaneously.

With increase of the head difference, the minimum effective height decreases, and the fresh groundwater discharge increases at the same dam location. Therefore, a steep head difference is beneficial to reducing engineering costs and reducing the accumulation of land-based pollutants and salt.

The reduction of the minimum effective dam height is conducive for saving engineering cost. Additionally, avoiding the reduction of the fresh groundwater discharge, as it is the case for a dam which is constructed over the whole aquifer thickness, decreases the accumulation of land-based pollutants and salt. Therefore, the site selection of the subsurface dams should consider both the engineering cost and ecological environmental effects. Tidal effects on the minimum effective dam height by changing the head difference (Luyun et al., 2009). Designers should carefully consider the minimum effective dam height on the lowest head difference (the head difference between the lowest underground water level and maximum tidal heights) in local history. An adequate safety margin should be reserved based on the minimum effective height. As this study firstly focussed on laboratory-scale setups, further studies will have to investigate field-scale implications to delineate minimum effective dam heights.

Acknowledgements This work was supported by the National Key Research and Development Program of China (No. 2016YFC0402810) and the National Natural Science Foundation of China-Shandong Joint Fund (No.U1806210) for funding this project.

References

Abarca, E., Vazquez-Sune, E., Carrera, J. et al., 2006. Optimal design of measures to correct seawater intrusion. Water Resources Research, 42(9).

Allow, K.A., 2012. The use of injection wells and a subsurface barrier in the prevention of seawater intrusion: a modelling approach. Arabian Journal of

Geosciences, 5(5), 1151-1161.

Abdoulhalik, A., Ahmed A.A., 2017a. The effectiveness of cutoff walls to control saltwater intrusion in multi-layered coastal aquifers: Experimental and numerical study. Journal of Environmental Management, 199, 62-73.

Abdoulhalik, A., Ahmed A.A., Hamill, G.A., 2017b. A new physical barrier system for seawater intrusion control. Journal of Hydrology, 549, 416-427.

Abdoulhalik, A., Ahmed, A.A., 2017c. How does layered heterogeneity affect the ability of subsurface dams to clean up coastal aquifers contaminated with seawater intrusion? Journal of Hydrology, 553, 708-721.

Bear, J., Cheng, A.H.D., Sorek, S., Ouazar, D., Herrera, I. (Eds.), 1999. Seawater Intrusion in Coastal Aquifers: Concepts, Methods and Practices. Springer Science & Business Media.

Botero-Acosta, A., Donado, L.D., 2015. Laboratory Scale Simulation of Hydraulic Barriers to Seawater Intrusion in Confined Coastal Aquifers Considering the Effects of Stratification. Procedia Environmental Sciences, 25, 36-43.

Cantalice, J.R.B., Piscoya, V.C., Singh, V.P., et al., 2016. Hydrology and water quality of a underground dam in a semiarid watershed. African Journal of Agricultural Research, 11(28), 2508–2518.

Goswami, R.R., Clement, T.P., 2007. Laboratory-scale investigation of saltwater intrusion dynamics. Water Resources Research, 43(4).

Hasan Basri, M., 2001. Two new methods for optimal design of subsurface barrier to control seawater intrusion, PhD thesis, The Univ. of Manitoba.

Ishida, S., Tsuchihara, T., Yoshimoto, S., et al., 2011. Sustainable use of groundwater with underground dams. Japan Agricultural Research Quarterly, 45(1), 51–61.

Jamali, I.A., Olofsson, B., Mörtberg, U., 2013. Locating suitable sites for the construction of subsurface dams using GIS. Environmental Earth Sciences, 70(6), 1-15.

Kaleris, V.K., Ziogas, A.I., 2013. The effect of cutoff walls on saltwater intrusion and groundwater extraction in coastal aquifers. Journal of Hydrology, 476, 370-383.

Kayode, O.T., Odukoya, A.M., Adagunodo, T.A., 2017. Saline Water Intrusion: Its Management and Control. Journal of Informatics and Mathematical Sciences, 9(2): 493-499.

Kang, P., Xu, S., 2017. The impact of an underground cut-off wall on nutrient dynamics in groundwater in the lower Wang River watershed, China. Isotopes in Environmental and Health Studies, 53(1), 36–53.

Guo, W., Langevin, C.D., 2002. User's Guide to SEAWAT: A Computer Program for Simulation of Three-Dimensional Variable-Density Groundwater Flow. US Geological Survey Techniques of Water Resources Investigations 6-A7. Tallahassee, Florida.

Goswami, R.R., Clement, T.P., 2007. Laboratory-scale investigation of saltwater intrusion dynamics. Water Resour. Res. 43, 1-11.

Langevin, C.D., 2003. Simulation of submarine ground water discharge to a marine estuary: Biscayne Bay, Florida. Ground Water, 41(6), 758–771.

Luyun, R., Momii, K., Nakagawa, K., 2009. Laboratory-scale saltwater behavior due to subsurface cutoff wall. Journal of Hydrology, 377(3-4), 227–236.

Luyun, R., Momii, K., Nakagawa, K., 2011. Effects of recharge wells and flow barriers on seawater intrusion. Ground Water, 49(2):239.

Lu, C.H., Chen, Y.M., Chang, Z., et al., 2013. Steady-state freshwater–seawater mixing zone in stratified coastal aquifers. Journal of Hydrology, 505, 24-34.

Luiz, D.S.G.J., Vieira, F.P., Mannathal, H.V., 2018. Use of electrical resistivity tomography in selection of sites for underground dams in a semiarid region in southeastern Brazil. Groundwater for Sustainable Development, S2352801X17301868.

Nawa, N., Miyazaki, K., 2009. The analysis of saltwater intrusion through Komesu underground dam and water quality management for salinity. Paddy and Water Environment, 7(2), 71–82.

Onder, H., Yilmaz, M., 2005. Underground Dams-A Tool of Sustainable Development and Management of Groundwater Resources. European Water, 11/12, 35-45.

Qu, W., Li, H., Huang, H., ., et al., 2017. Seawater-groundwater exchange and nutrients carried by submarine groundwater discharge in different types of wetlands at Jiaozhou Bay, China. Journal of Hydrology, 555, 185–197.

Raju, N.J., Reddy, T.V.K., Muniratnam, P., et al., 2013. Managed aquifer recharge

(MAR) by the construction of subsurface dams in the semi-arid regions: A case study of the Kalangi river basin, Andhra Pradesh. Journal of The Geological Society Of India, 82(6), 657-665.

Silva, M.S.L.D., Lopes, P.R.C., Anjos, J.B.D., 1998. Agricultural exploration on underground dams. Pesquisa Agropecuaria Brasileira.

Sugio, S., Nakada, K., Urish, D.W., 1987. Subsurface seawater intrusion barrier analysis. Journal of Hydraulic Engineering, 6(113), 767-779.

Shoemaker, W.B., 2004. Important observations and parameters for a salt water intrusion model. Ground Water, 42 (6), 829–840.

Senthilkumar, M., Elango, L., 2011. Modelling the impact of a subsurface barrier on groundwater flow in the lower Palar River basin, southern India. Hydrogeology Journal, 19(4), 917-928.

Sun, D.M., Semprich, S., 2013. Using Compressed Air Injection to Control Seawater Intrusion in a Confined Coastal Aquifer. Transport in Porous Media, 100(2), 259-278.

Stevanović, Z., 2015. Damming underground flow to enhance recharge of karst aquifers in the arid and semi-arid worlds. Environmental Earth Sciences, 75(1), 35.

Stoeckl, L., Walther, M., Graf, T., 2016. A new numerical benchmark of a freshwater lens. Water Resources Research 52, 2474–2489.

Sathe S. S., & Mahanta C., 2019. Groundwater flow and arsenic contamination transport modeling for a multi aquifer terrain: Assessment and mitigation strategies. Journal of Environmental Management, 231, 166–181.

Sun, Q.G., Zheng, T.Y., Zheng. X.L., et al., 2019. Influence of a subsurface cut-off wall on nitrate contamination in an unconfined aquifer. Journal of Hydrology, 575, 234-243.

Tavakoli-Kivi, S., Bailey, R. T., Gates, T. K., 2019. A Salinity Reactive Transport and Equilibrium Chemistry Model for Regional-Scale Agricultural Groundwater Systems. Journal of Hydrology, 572, 274–293.

Voss, C.I., Souza, W.R, 1987. Variable density flow and solute transport simulation of regional aquifers containing a narrow freshwater-saltwater transition zone. Water Resources Research, 23, 1851-1866.

Werner, A.D., Bakker, M., Post, V.E.A., Vandenbohede, A., Lu, C., Ataie-Ashtiani, B., Barry, D.A., 2013. Seawater intrusion processes, investigation and management: Recent advances and future challenges. Advances in Water Resources, 51, 3-26.

Walther, M., Graf, T., Kolditz, O., et al., 2017. How significant is the slope of the sea-side boundary for modelling seawater intrusion in coastal aquifers? Journal of Hydrology, 551, 648–659.

Yasumoto, J., Nakano, T., Nawa, N., 2011. Underground dams for irrigation supplies in coastal limestone aquifer, Okinawa, Japan. AGU Fall Meeting Abstracts.

Yu, L., Wu, X.Q., Zheng, X.L., et al., 2019. An index system constructed for ecological stress assessment of the coastal zone: A case study of Shandong, China, Journal of Environmental Management, 232, 499-504.

Zhang, B., Zheng, X.L., Zheng, T.Y., et al., 2019. The influence of slope collapse on water exchange between a pit lake and a heterogeneous aquifer. Frontiers of Environmental Science & Engineering, 13(2), 20.